Quantum properties of a strongly interacting frustrated disordered magnet

James W. Landry*
Sandia National Laboratories, Albuquerque, New Mexico 87185-1415, USA

S. N. Coppersmith†
Physics Department, University of Wisconsin, 1150 University Avenue, Madison, Wisconsin 53706, USA
(Received 21 September 2003; revised manuscript received 22 December 2003; published 26 May 2004)

We compute the low-energy quantum states and low-frequency dynamical susceptibility of a quantum generalization of the two-dimensional Edwards-Anderson spin glass, obtaining exact numerical results for system sizes much larger than previously accessible. The ground state is a complex superposition of a substantial fraction of all the classical ground states, often having large connected regions of spins all exhibiting strong quantum fluctuations, and yet the dynamical susceptibility exhibits sharp resonances reminiscent of the behavior of single spins. The dependence of the energy spectra on system size differs qualitatively from that of the energy spectra of random undirected bipartite graphs with similar statistics, implying that strong interactions are giving rise to these unusual spectral properties.

DOI: 10.1103/PhysRevB.69.184416 PACS number(s): 75.50.Lk, 75.10.Nr

I. INTRODUCTION

The promise and difficulty of quantum dynamics both arise because the amount of information needed to specify a quantum state grows exponentially with the system size—2^N complex numbers are needed to specify a general quantum state of N quantum-mechanical two-state spins (or qubits). A classical computer performing 10^{14} floating point operations per second[1] would take 10^8 years to perform a single operation on the state when $N=100$ and 10^{21} years when $N=144$.

Here we study a frustrated spin model that is a quantum generalization of the two-dimensional $\pm J$ Edwards-Anderson (EA) spin-glass model,[2] a canonical example of a classical system whose competing interactions give rise to many low-energy states. The essential physical ingredients of the EA model arise in a wide variety of optimization problems in many fields:[3] the system cannot satisfy simultaneously all its constraints, and many different configurations are equally effective in minimizing the energy. Though the two-dimensional $\pm J$ EA model is simpler than the three-dimensional version—it is disordered at all nonzero temperatures[4] and individual ground states can be found in a time that scales polynomially with system size[5]—it has a large ground-state degeneracy and a complex energy landscape.[4,6,7] We study the quantum system obtained by adding a small quantum tunneling term to the two-dimensional $\pm J$ EA model.

By exploiting a fast algorithm for finding all the ground states of the classical model,[8] we calculate numerically exact eigenstates and dynamical response functions of quantum EA models with up to 144 spins in the limit of strong interaction strength. The quantum ground states typically have substantial connected regions of spins all exhibiting strong quantum fluctuations, and yet at low frequencies the excitation spectrum is remarkably sparse. The number of excitations per unit energy at low energies does not vary significantly with system size, even though the number of eigenvalues grows exponentially with system size while the energy bandwidth only grows polynomially. The eigenvalues and eigenvectors of each realization are obtained by diagonalizing the adjacency matrix of a graph, and we demonstrate that strong correlations play a vital role by comparing the spin-glass excitation spectra to spectra of graphs with similar connectivity statistics but randomly chosen connections.

The paper is organized as follows. Section II defines the model and the calculational method, Sec. III describes the results, and Sec. IV discusses the results and their possible relationship to recent experimental observations of the dynamical behavior of the quantum spin liquid $LiY_{0.955}Ho_{0.045}F_4$.[9]

II. MODEL AND METHODS

We study two-dimensional systems with periodic boundary conditions in which spin-1/2 spins interact with nearest neighbors on $\sqrt{N}\times\sqrt{N}$ square lattices. The quantum Hamiltonian is

$$H_Q = -\sum_{\langle ij\rangle} J_{ij}\sigma_{i,z}\sigma_{j,z} + \Gamma\sum_i \sigma_{i,x}, \tag{1}$$

where $\sigma_{i,x}$ and $\sigma_{i,z}$ are Pauli matrices: $\sigma_{i,x}=\left(\begin{smallmatrix}0&1\\1&0\end{smallmatrix}\right)$ and $\sigma_{i,z}=\left(\begin{smallmatrix}1&0\\0&-1\end{smallmatrix}\right)$. The sum $\langle ij\rangle$ is over all nearest neighbor pairs. A given sample has a fixed realization of bonds in which each bond J_{ij} is chosen to be $-J$ and $+J$ with equal probability. This Hamiltonian, which has been studied by many groups,[10] is believed to have relevance to the experimental system $LiY_xHo_{1-x}F_4$,[9,11,12] where the coefficient Γ is tunable because it is proportional to an applied transverse magnetic field. The $\Gamma\to 0$ limit is the two-dimensional $\pm J$ EA model.[2]

The calculation uses standard degenerate perturbation theory[13] to compute the low-energy quantum states. We set the energy zero to be the ground-state energy of the classical model. The diagonal terms of the Hamiltonian matrix are the classical energies of the different configurations—zero for the ground states, $4J$ for the first excited states, etc. The off-diagonal terms describing the transitions between these configurations are just Γ, so they do not depend on J at all. As $\Gamma/J\to 0$ the contribution to the quantum ground state by

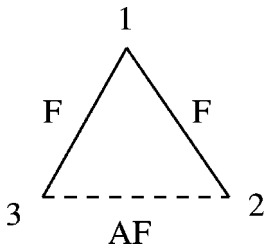

FIG. 1. Three-spin example used to illustrate method.

states that are not classical ground states tends to zero, and the low-energy quantum states $|\psi_n\rangle$ become superpositions of states corresponding to ground-state configurations $|\alpha\rangle$ of the classical model,

$$|\psi_n\rangle = \sum_\alpha c_{\alpha n}|\alpha\rangle. \tag{2}$$

Therefore, in the strongly interacting limit $\Gamma \to 0$ the quantum ground state can be obtained if one can find *all* the ground states of the classical model. To illustrate the procedure, consider the simple three-spin triangle shown in Fig. 1. The spins are connected by three bonds, two ferromagnetic and one antiferromagnetic.[32] This system has eight classical configurations: ($|\uparrow\uparrow\uparrow\rangle$, $|\uparrow\uparrow\downarrow\rangle$, $|\uparrow\downarrow\uparrow\rangle$, $|\downarrow\uparrow\downarrow\rangle$, $|\downarrow\downarrow\uparrow\rangle$, $|\downarrow\downarrow\downarrow\rangle$, $|\uparrow\downarrow\downarrow\rangle$, and $|\downarrow\uparrow\uparrow\rangle$). With the energy zero set as the classical ground-state energy, the first six configurations have classical energy $E=0$, and the final two configurations have classical energy $E=4J$. The Hamiltonian matrix using the basis

$$\begin{pmatrix} |\uparrow\uparrow\uparrow\rangle \\ |\uparrow\uparrow\downarrow\rangle \\ |\uparrow\downarrow\uparrow\rangle \\ |\downarrow\uparrow\downarrow\rangle \\ |\downarrow\downarrow\uparrow\rangle \\ |\downarrow\downarrow\downarrow\rangle \\ |\uparrow\downarrow\downarrow\rangle \\ |\downarrow\uparrow\uparrow\rangle \end{pmatrix} \tag{3}$$

is

$$\begin{pmatrix} 0 & \Gamma & \Gamma & 0 & 0 & 0 & 0 & \Gamma \\ \Gamma & 0 & 0 & \Gamma & 0 & 0 & \Gamma & 0 \\ \Gamma & 0 & 0 & 0 & \Gamma & 0 & \Gamma & 0 \\ 0 & \Gamma & 0 & 0 & 0 & \Gamma & 0 & \Gamma \\ 0 & 0 & \Gamma & 0 & 0 & \Gamma & 0 & \Gamma \\ 0 & 0 & 0 & \Gamma & \Gamma & 0 & \Gamma & 0 \\ 0 & \Gamma & \Gamma & 0 & 0 & \Gamma & 4J & 0 \\ \Gamma & 0 & 0 & \Gamma & \Gamma & 0 & 0 & 4J \end{pmatrix}. \tag{4}$$

Standard degenerate perturbation theory to lowest (linear) order in Γ/J consists of discarding the rows and columns for configurations with nonzero classical energy from the Hamiltonian matrix.[33]

The number of ground states of the classical two-dimensional $\pm J$ EA model grows with N much more slowly than the number of configurations (though still exponentially).[6,8] For each realization, we find all ground states of the classical system using the algorithm of Ref. 8. All ground states are found, in contrast to previous work where only a few ground states were determined.[14] Before the work in Ref. 8, there was no efficient, reliable method to determine all the ground states of these systems, so enumeration of ground states was limited to very small systems of $N=16$ or smaller. The requirement that all classical ground states must be obtained naturally limits the size of the systems we may consider, since the number of ground states grows exponentially with system size. However, finding *all* the classical ground states is necessary for obtaining the quantum ground state.

We studied randomly generated system realizations with equal numbers of ferromagnetic and antiferromagnetic bonds and periodic boundary conditions. We only computed the quantum states for systems with less than 400 000 classical ground states; in principle this cutoff could have been increased slightly (but not greatly because of memory limits), but at the cost of much slower computations. Performing the computations for realizations with 400 000 classical ground states typically took a few days on a 1 GHz PC. Because the distribution of the number of ground states is log-normal,[6,8] some realizations have orders of magnitude more ground states than the mean for the given system size. For $N=64$, for a sample of 1000 realizations, the median number of classical ground states was 568, and 997/1000 realizations had less than 400 000 classical ground states, our upper cutoff size. For $N=100$, for 1000 realizations the median number of classical ground states was 9461, with 901/1000 realizations having less than 400 000 classical ground states. For $N=144$, for 100 realizations the median number of classical ground states was 409 794, and 49/100 realizations had less than 400 000 classical ground states.

Once the complete set of classical ground states is determined for a given realization, we use standard degenerate perturbation theory[13] to compute the low-energy quantum states. In the limit $\Gamma/J \to 0$, each low-energy quantum eigenstate is a superposition of classical ground-state configurations related to each other by serial flipping of individual flippable spins, where a flippable spin is one with an equal number of satisfied and unsatisfied bonds.[15] Changing a flippable spin from up to down or vice versa has no effect on the total energy. We thus construct the quantum tunneling matrix with elements $\langle\alpha|(\Sigma_i \sigma_{ix})|\beta\rangle$, where the basis states $|\alpha\rangle$ and $|\beta\rangle$ are classical ground states. The matrix element is nonzero only if the two states differ by a single spin flip. To lowest order, only states $|\alpha\rangle$ and $|\beta\rangle$ with the same energy contribute, which means that the single spin flip must be of a flippable spin. Since the number of flippable spins clearly cannot exceed N, the number of spins in the system, and the number of ground states grows exponentially with N, the

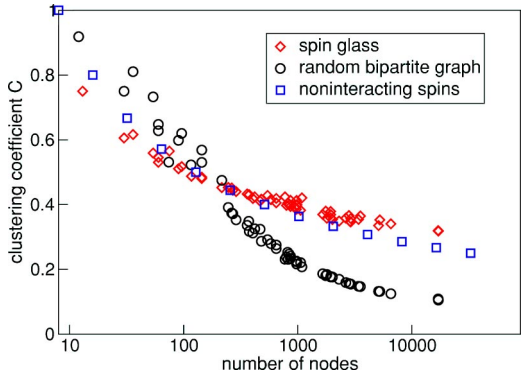

FIG. 2. Clustering coefficients C of spin-glass graphs, of bipartite random graphs with the same number of nodes and edges, and of graphs for noninteracting quantum spins, vs number of nodes. The clustering coefficients of the spin-glass graphs are significantly larger than those of random bipartite graphs, and close to those of graphs for noninteracting spins.

matrix of possible transitions between classical ground states is extremely sparse, and thus well suited for diagonalization using Lanczos techniques.[16–18] To compute the dynamical magnetic susceptibility, we find low-energy eigenvalues and eigenstates using the sparse matrix ARPACK numerical library[19] with C++ bindings.[20]

When the Hilbert space is truncated so that it includes only classical ground states, the quantum energies are proportional to Γ. Including the configurations with higher classical energy lead to corrections to this linear-in-Γ behavior that are higher order in Γ/J; we expect these corrections to be small so long as the energy arising from the quantum perturbation ($\lesssim \Gamma N$) is smaller than the energy gap between the classical ground state and lowest classical excited states ($=J$), so that the procedure is valid only for $\Gamma \lesssim J/N$. Exact diagonalizations of very small (3×3 and 4×4) systems are consistent with this expectation.

III. RESULTS

It is difficult to obtain meaningful averages over disorder for this system because for a given system size there are enormous sample-to-sample variations in the number of classical ground states in the classical model.[8] We have found it useful to subdivide the sampling further by keeping track of the number of classical ground states for each realization. The usefulness of this subdivision is illustrated by Fig. 2, which shows the clustering coefficients (defined below) for about one-hundred 10×10 realizations. The clustering coefficient varies by over a factor of 2, but the figure demonstrates that most of this variation is due to a systematic dependence of the clustering feature on the number of classical ground states or nodes. However, considering systems with the same number of classical ground states does not remove all the variability between realizations. This point is illustrated by Fig. 3(b), which shows three different realizations with similar numbers of classical ground states but different numbers of bunches, which are defined as contiguous sets of flippable spins.[8] Bunches are significant because they are independent in the sense that the set of different classical ground states is given by all possible combinations of the different ground states of the individual bunches. There is significant variability in the number of bunches and of their sizes, as illustrated by the three realizations shown, which systems have four bunches, nine bunches, and one bunch, respectively. The spectra and clustering coefficients for all three of these cases are qualitatively similar, but the participation ratios (defined below) for the three cases do differ significantly.

The ground-state dynamical magnetic susceptibility $\chi''(\omega)$ characterizes the response of a system at zero temperature to a magnetic field applied along z oscillating at angular frequency ω.[21] The susceptibility consists of sets of Dirac δ-function peaks (that in physical systems spread out into a finite width in frequency due to decoherence processes); $\hbar\omega$ for each peak is the energy difference between an excited state and the ground state. For the $\pm J$ spin glass, as $\Gamma/J \to 0$ the value of J affects only the energy zero and the susceptibility at frequencies ω satisfying $\hbar\omega \ll J$ depends only on the ratio $\hbar\omega/\Gamma$.

Figure 4 shows the zero-temperature dynamic magnetic susceptibility of systems of size 6×6, 8×8, 10×10, and 12×12. The density of low-energy excitations increases extremely slowly with system size. This result is surprising because the number of energy eigenvalues grows exponentially with the number of spins N, while these energies all lie within a bandwidth that grows roughly linearly with N.

To obtain context for these results, we interpret the Hamiltonian matrix for the quantum spin glass as the adjacency matrix of an undirected bipartite graph[22–24] in which each classical ground state is a node and edges connect every pair of classical ground states coupled by the quantum term in the Hamiltonian. The graph is bipartite because the edges connect states that differ by a single spin reversal, one of which has an even and the other an odd number of up spins. The spin-glass graphs have a modest number of disconnected pieces called clusters.[25] Figure 5 compares the density of energy levels of the largest cluster of a 10×10 spin-glass realization (with 17 040 nodes and 77 684 edges) to the density of energy levels of a symmetric bipartite random matrix with 10 000 nodes and 50 000 edges. The random bipartite matrices are constructed by dividing the nodes into two groups of equal size. First, each node is connected to a randomly chosen node in the other group (this ensures that the graph has no disconnected pieces), and then links are added between a randomly chosen vertex in each group until the total number of edges is reached. The bipartite random matrix has a large energy gap between the ground state and first excited state, and once this gap is exceeded the density of energy levels is much greater than at low energies in the spin glass. The energy-level spacing between the excited states of the random matrix is approximately inversely proportional to the number of nodes.

We have compared other properties[26] of the graphs underlying the quantum spin glass to those of random bipartite graphs. The degree distribution[27] describing the number of links emanating from the nodes of the spin-glass graphs is even narrower than the Poisson distribution of a bipartite random graph with the same mean degree. Figure 2 shows

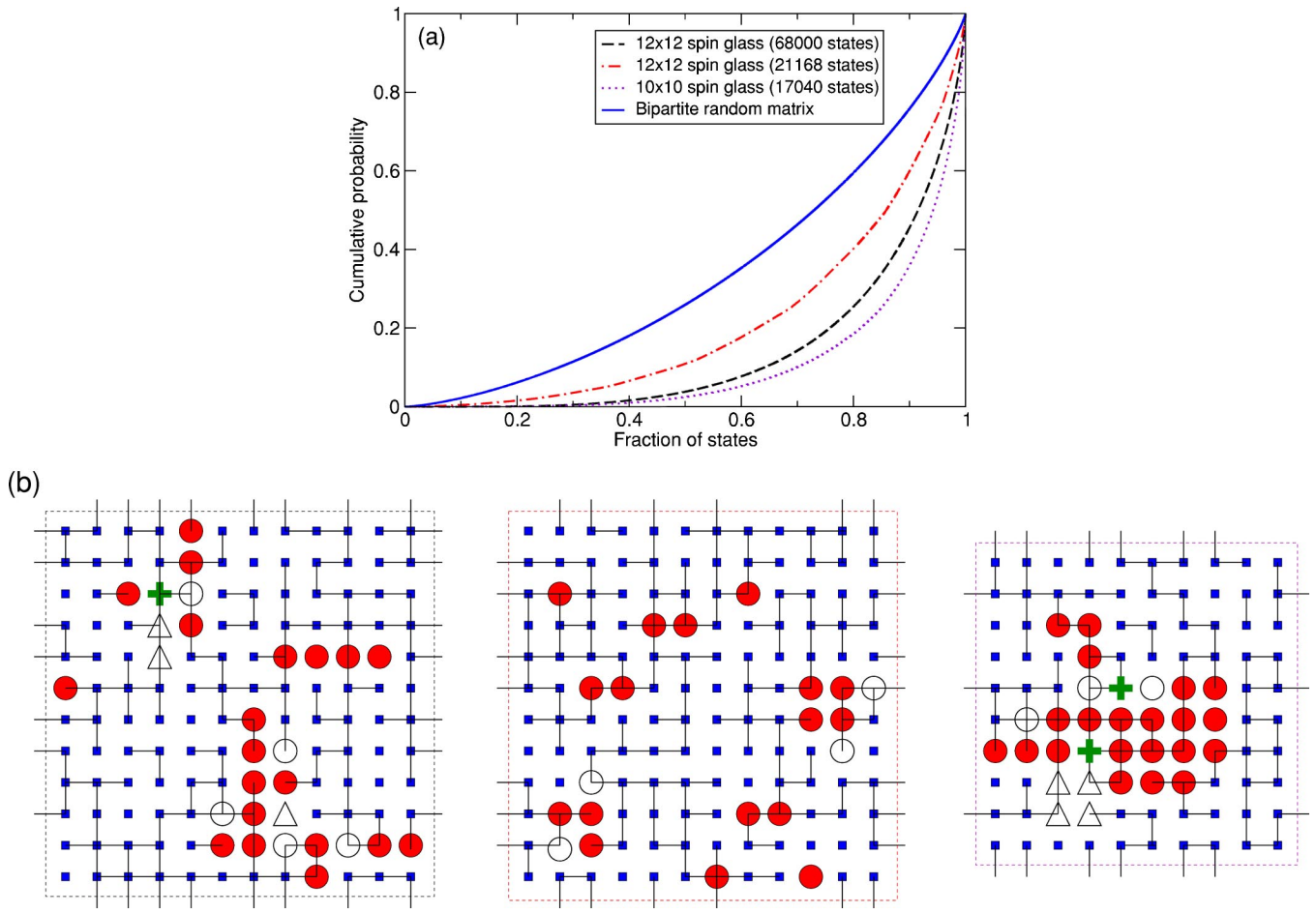

FIG. 3. (a) Cumulative probability of the sorted participation ratios P_α for three-spin-glass realizations and for bipartite random graphs. Here, $P_\alpha=|c_{\alpha 0}|^2$, with the $c_{\alpha n}$ defined in Eq. (2). The number of states contributing 50% and 100% of the total probability are 2996/21 168, 5762/68 000, and 986/17 040. The spin-glass participation ratios are significantly less evenly distributed than for the random bipartite graph; still, many spin-glass configurations contribute significantly to the quantum ground state. (b) Flippable spins in the quantum ground state of three different realizations of bonds. Spins denoted by △ have $|\langle S_i\rangle|<1$, + for $|\langle S_i\rangle|<0.999$, ○ for $|\langle S_i\rangle|<0.99$, and ● for $|\langle S_i\rangle|<0.9$. The black lines denote antiferromagnetic bonds connecting the spin sites. The quantum ground state has relatively large contiguous clusters of spins that exhibit strong quantum fluctuations, so it cannot be thought of as noninteracting isolated "free" spins.

the clustering coefficient C,[28] which for bipartite graphs is the probability that two nodes with a common second neighbor are themselves second neighbors.[29] The clustering coefficients of spin-glass graphs are significantly larger than those of bipartite random graphs with the same number of nodes and edges,[29] and are close to those of graphs describing N noninteracting spins, which have 2^N nodes, each node with degree N, and clustering coefficients $C=4/(N+1)$ (see Appendix). This result demonstrates that the graphs underlying the quantum spin glass have local connectivity properties that differ significantly from random graphs. Thus, both local (clustering coefficients) and nonlocal properties (eigenvalue spectra) of the graphs reflect correlations induced by the energy minimization procedure.

Though some statistical properties of the spin-glass graphs are similar to those of graphs for noninteracting quantum spins, the ground state of the quantum spin glass differs significantly from that of noninteracting quantum spins. This point is illustrated by Fig. 3(b), which displays for three different realizations (the 10×10 realization is the same as that in Fig. 5) the flippable spins in the quantum ground state. Shown are the spins with $|\langle S_{iz}\rangle|<0.9$, 0.99, 0.999, and 1, where $\langle S_{iz}\rangle$ is the expectation value of the zth component of the ith spin. The figure demonstrates that the ground state has a relatively large connected region of strongly fluctuating spins. Figure 3(a) shows the cumulative probability of the participation ratios P_α of different classical ground states in the quantum ground state, where $P_\alpha=|c_{\alpha 0}|^2$, with the $c_{\alpha 0}$ defined in Eq. (2). The spin-glass participation ratios differ both from those of a bipartite random matrix and those of N noninteracting quantum spins, whose cumulative probability is a straight line (since the participation ratio is $1/2^N$ for all classical configurations). For the spin glass, between 5% and 14% of the states contribute 50% of the probability, indicating that many classical basis states contribute significantly to the quantum ground state.

IV. DISCUSSION

Our results demonstrate that typical ground states of two-dimensional $\pm J$ Ising spin glasses with quantum tunneling

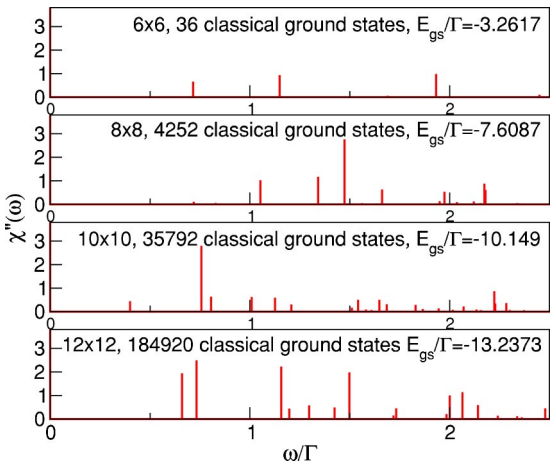

FIG. 4. Zero-temperature dynamic magnetic susceptibility $\chi''(\omega)$ of systems of size 6×6, 8×8, 10×10, and 12×12. The peaks in the susceptibility occur at frequencies ω that satisfy $\hbar\omega = E_n - E_0$, where E_n is the energy of an excited state and E_0 is the energy of the ground state. The density of low-energy excitations does not increase appreciably as the system size increases, even though an exponentially increasing number of states are in an energy bandwidth that grows approximately linearly with the system size.

cannot be viewed simply as a collection of isolated two-state systems, and yet nonetheless the density of low-energy excitations is very low. We expect the sparse spectrum at low energies to lead to saturable dynamical response, since if a perturbation induces a resonant transition from the ground state to an excited state, in general the perturbation is not resonant for a transition from the excited state to a third state of higher energy. The experimental signature of spectra of this type is the observation of hole burning, where application of a perturbation at a given frequency results in suppression of the response at this frequency.[30] Indeed, sharp, saturable resonances resulting in hole-burning have been found experimentally in the quantum spin liquid $LiY_{0.955}Ho_{0.045}F_4$.[9] However, the model we study differs significantly from the experimental system in important ways—it is a two-dimensional model with specially tuned short-range interactions, while the experimental system is a three-dimensional system with dipolar interactions. Unfortunately, generalizing our methods to three-dimensional systems and to systems with long-range interactions is computationally prohibitive.

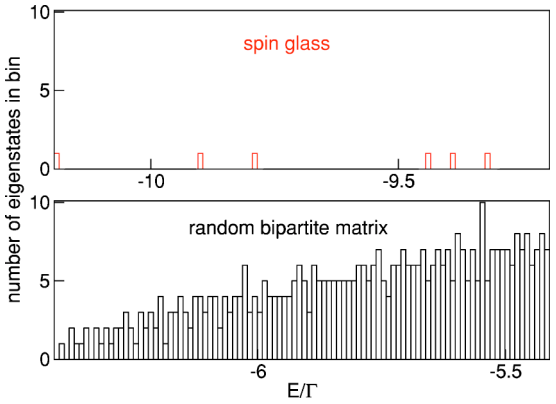

FIG. 5. Density of states as a function of energy at low energies for the largest connected component (with 17 040 nodes and 77 684 links) of the graph characterizing a 10×10 spin glass realization and of a bipartite random matrix with 10 000 nodes and 50 000 links. The quantum ground-state energy E_0 for the spin glass is $E_0/\Gamma = -10.1949$, and for the bipartite graph $E_0/\Gamma = -10.2335$. The ordinate shows the number of eigenvalues in a bin of width 0.01. The bipartite random matrix has a large gap between the ground state and first excited state, and, once the gap is exceeded, a much larger density of states than the spin glass.

ACKNOWLEDGMENTS

We have benefited greatly from discussions with J. Brooke, S. Ghosh, T. F. Rosenbaum, S. Sabhapandit, and S. A. Trugman. This work was supported by the MRSEC program of the National Science Foundation under Grant No. DMR-9808595 at The University of Chicago by the Petroleum Research Fund of the American Chemical Society, and by the National Science Foundation under Grant No. DMR-0209630. Sandia is a multiprogram laboratory operated by Sandia Corporation, a Lockheed Martin Company, for the United States Department of Energy under Contract No. DE-AC04-94AL85000. S.N.C. thanks the Aspen Center for Physics for hospitality during the preparation of this manuscript.

APPENDIX: CLUSTERING COEFFICIENT FOR GRAPHS DESCRIBING NONINTERACTING QUANTUM SPINS

The clustering coefficient C is defined as the fraction of pairs of states that are second neighbors to a reference state that are also second neighbors to each other. To calculate C for the graph for noninteracting quantum spins, first we find the number of pairs of distinct second neighbors of a given reference state. By symmetry, all states are equivalent, so one can without loss of generality assume that the reference state has all spins up. All second neighbors to this reference state have two spins down, which can occur in $M = N(N-1)/2$ distinct ways. The number of distinct pairs of second neighbors is $M(M-1)/2$, or $\frac{1}{2}[\frac{1}{2}N(N-1)][\frac{1}{2}N(N-1)-1]$. To count the number of pairs of states that are second neighbors to the reference state and also second neighbors to each other, we note that each state in the pair has two spins that differ from the reference state, and they are second neighbors to each other if one of these spins is in common. For a given reference state, there are $N(N-1)/2$ ways to choose the first state of the pair. If the second state of the pair is a second neighbor, then one of the two flipped spins is the same in the second state of the pair also. There are $N-2$ possible locations of the second flipped spin in the second state, since it can be anywhere except for the locations of the two flipped

spins of the first state of the pair. Each pair is counted twice by this process, so the number of ways to choose a pair of states that are second neighbors to each other as well as the reference state is $(\frac{1}{2})[\frac{1}{2}N(N-1)](2)(N-2)$, and the clustering coefficient C is

$$C=\frac{\left(\frac{1}{2}\right)\left[\frac{1}{2}N(N-1)\right](2)(N-2)}{\frac{1}{2}\left[\frac{1}{2}N(N-1)\right]\left[\frac{1}{2}N(N-1)-1\right]}=\frac{4}{N+1}. \quad \text{(A1)}$$

*Electronic address: jwlandr@sandia.gov
†Electronic address: snc@physics.wisc.edu

[1] The world's fastest supercomputer performs slightly fewer than 4×10^{13} floating point operations per second (http://www.top500.org/).
[2] S. Edwards and P. Anderson, J. Phys. F: Met. Phys. **5**, 965 (1975).
[3] M. Mezard, G. Parisi, and M. Virasoro, *Spin Glass Theory and Beyond: An Introduction to the Replica Method and Its Applications* (World Scientific, Singapore, 1987).
[4] M. Palassini and A. Young, Phys. Rev. B **63**, 140408(R) (2001).
[5] L. Bieche, J. Uhry, R. Maynard, and R. Rammal, J. Phys. A **13**, 2553 (1980).
[6] L. Saul and M. Kardar, Phys. Rev. E **48**, R3221 (1993); Nucl. Phys. B **432**, 641 (1994).
[7] G. Santoro, R. Martonak, E. Tosatti, and R. Car, Science **295**, 2427 (2002).
[8] J. Landry and S. Coppersmith, Phys. Rev. B **65**, 134404 (2002).
[9] S. Ghosh, R. Parthasarathy, T. Rosenbaum, and G. Aeppli, Science **296**, 2195 (2002).
[10] M. Guo, R. Bhatt, and D. Huse, Phys. Rev. Lett. **72**, 4137 (1994); H. Rieger and A. Young, *ibid.* **72**, 4141 (1994); D. Fisher, Phys. Rev. B **51**, 6411 (1995); C. Pich, A. Young, H. Rieger, and N. Kawashima, Phys. Rev. Lett. **81**, 5916 (1998); D.A. Huse, Phys. Rep. **348**, 149 (2001); F. Igloi, Phys. Rev. B **65**, 064416 (2002).
[11] J. Brooke, D. Bitko, T. Rosenbaum, and G. Aeppli, Science **284**, 779 (1999).
[12] J. Brooke, T. Rosenbaum, and G. Aeppli, Nature (London) **413**, 610 (2001).
[13] R. Shankar, *Principles of Quantum Mechanics* (Plenum Press, New York, 1980).
[14] A. Hartmann and A. Young, Phys. Rev. E **64**, 180404 (2001).
[15] S. Coppersmith, Phys. Rev. Lett. **67**, 2315 (1991).
[16] J. Cullum and R. Willoughby, *Lanczos Algorithms for Large Symmetric Eigenvalue Computations: Theory* (Birkhauser, Boston, MA, 1985).
[17] E. Dagotto, Rev. Mod. Phys. **66**, 763 (1994).
[18] C. Lanczos, *Linear Differential Operators, Classics in Applied Mathematics*, Vol. 18 (Society for Industrial and Applied Mathematics, Philadelphia, 1996).
[19] R. Lehoucq, K. Maschhoff, D. Sorensen, and C. Yang, http://www.caam.rice.edu/software/ARPACK/
[20] S. Shaw, http:// monsoon.harvard.edu/~shaw/programs/lapack.html
[21] The ground-state dynamical magnetic susceptibility is

$$\chi''(\omega)=\sum_n |\langle\psi_n|M_z|\psi_0\rangle|^2\delta(\omega-\omega_{n0}),$$

where the sum is over quantum energy eigenstates $|\psi_n\rangle$, $|\psi_0\rangle$ is the quantum ground state, $\hbar\omega_{n0}=(E_n-E_0)$ is the energy difference between the states $|\psi_n\rangle$ and $|\psi_0\rangle$, and $M_z=\Sigma_\alpha\sigma_{\alpha z}$ is the z component of the total magnetization [see, e.g., E.R. Gagliano and C.A. Balseiro, Phys. Rev. B **38**, 11 766 (1988)].
[22] G. Chartrand, *Introductory Graph Theory* (Dover, New York, 1985).
[23] D. Cvetkovic, M. Doob, and H. Sachs, *Spectra of Graphs: Theory and Application* (Academic Press, New York, 1980).
[24] I. Farkas, I. Derenyi, A.-L. Barabasi, and T. Vicsek, Phys. Rev. E **64**, 026704 (2001).
[25] A. Hartmann, Phys. Rev. E **63**, 016106 (2001).
[26] R. Albert and A.-L. Barabasi, Rev. Mod. Phys. **74**, 47 (2002).
[27] A.-L. Barabasi and R. Albert, Science **286**, 509 (1999).
[28] D. Watts and S. Strogatz, Nature (London) **393**, 440 (1998).
[29] M. Newman, S. Strogatz, and D. Watts, Phys. Rev. E **64**, 026118 (2001).
[30] W. E. Moerner, *Persistent Spectral Hole-Burning: Science and Application*, Springer Topics in Current Physics, Vol. 44 (Springer-Verlag, New York, 1988).
[31] J. Schrieffer and P. Wolff, Phys. Rev. **149**, 491 (1966).
[32] Higher-order corrections may be obtained in principle via canonical transformation (Ref. 31).
[33] The triangular lattice was chosen for this example to minimize the number of spins. All systems considered in this study were square lattices.